Journal of
Nanoelectronics and Optoelectronics
Vol. 14, pp. 1–8, 2019
www.aspbs.com/jno

ARTICLE

Electronic and Optical Properties of the Spinel Oxides GeB_2O_4 (B = Mg, Zn and Cd): An *Ab-Initio* Study

Djamel Allali[1, 2, *], Abdelmadjid Bouhemadou[3], Fares Zerarga[4], and Foudil Sahnoune[1]

We report *ab-initio* density functional theory calculations of the electronic and optical properties of the spinel oxides $GeMg_2O_4$, $GeZng_2O_4$ and $GeCd_2O_4$ using the full potential linearized augmented plane-wave method. To calculate the electronic properties, the exchange-correlation interaction was treated with various functionals. We find that the newly developed Tran–Blaha modified Becke–Johnson functional significantly improves the band gap value. All considered GeB_2O_4 compounds are direct band gap materials. The band gap value decreases with increasing atomic size of the B element. The decrease of the fundamental direct band gap (Γ–Γ) when one moves from $GeMg_2O_4$ to $GeZn_2O_4$ to $GeCd_2O_4$ can be attributed to the *p*–*d* mixing in the upper valence bands of $GeZn_2O_4$ and $GeCd_2O_4$. The lowest conduction band, which is mainly originated from the *s* and *p* states of the Ge and B (B = Mg, Zn, Cd) atoms, is well dispersive, similar to that of transparent conducting oxides such as ZnO. The topmost valence band, which is originated from the O-2*p* and B-*d* states, is considerably less dispersive. Optical spectra in a wide energy range from 0 to 30 eV are provided and the origin of the observed peaks and structures are assigned. We find that the zero-frequency limit of the dielectric function $\varepsilon(0)$ increases with decreasing band gap value.

Keywords: Semiconductor, *Ab Initio* Calculation, Optical Properties, Electronic Structure.

1. INTRODUCTION

Spinel oxides with the chemical formula AB_2O_4 form a family of ∼120 compounds. In the spinel oxide AB_2O_4, the cation A (B) is either divalent (trivalent) ($A^{II}B^{III}_2O_4$: A^{II} = Cd, Mg, Mn, Zn…, and B^{III} = Al, Ga, In…) or tetravalent (divalent) ($A^{IV}B^{II}_2O_4$: A^{IV} = Si, Ge, Sn…, and B^{II} = Cd, Mg, Mn, Zn…). The cation A is surrounded by four oxygen ions, forming an AO_4 tetrahedron, whereas the cation B is surrounded by six oxygen ions, forming an edge-sharing BO_6 octahedron (see Fig. 1). Spinel oxides AB_2O_4 crystalize in a cubic close packing (FCC) lattice with the $Fd\bar{3}m$ (n. 227) space group symmetry. The AB_2O_4 unit cell contains 56 atoms or eight unit formulas (8 AB_2O_4) [1, 2]. Spinel oxides possess many interesting electronic, mechanical, magnetic, and optical properties, which make them potential candidate materials for numerous technological applications. Therefore, these materials have been the subject of numerous experimental and theoretical studies [3–9]. Among their interesting properties, the electronic and optical properties have especially attracted considerable attention because the knowledge of these properties is required to know if these materials are potential candidates for eventual applications in optoelectronic devices.

Recent growing demand for high-performance and low-cost transparent conducting oxides (TCOs) in optoelectronic devices, such as flat-panel displays, windshield defrosters and solar cells [10], has led to an extensive search for new TCO materials with higher transparency and conductivity [3]. There has been a considerable work involving both experimental and theoretical methods on the $A^{II}B^{V}_2O_4$ spinel oxides, such as $MgAl_2O_4$, $ZnAl_2O_4$ and $ZnGa_2O_4$ [3–5]. However, there are very few reports on the $A^{IV}B^{II}_2O_4$ spinel oxides, such as

[1]University of M'sila, Physics and Chemistry of Materials Lab, Faculty of Science, Department of Physics, 28000, Algeria
[2]University of M'sila, Faculty of Technology, B.P. 166 Ichbilia, 28000, M'sıla, Algeria
[3]Laboratory for Developing New Materials and Their Characterizations, University Ferhat Abbas Setif 1, 19000, Algeria
[4]University Abderrahmane Mira, Department of Physics, Bejaia, 06000, Algeria
*Author to whom correspondence should be addressed.
Email: djamel.allali@univ-msila.dz
Received: 16 October 2018
Accepted: 13 December 2018

$GeMg_2O_4$, $GeZn_2O_4$ and $GeCd_2O_4$. Apart their structural properties [4, 11], elastic constants [11], and electronic structure properties [11], some fundamental properties of the $GeMg_2O_4$, $GeZn_2O_4$, and $GeCd_2O_4$ compounds are not yet investigated. We are not aware of any studies on their optical properties. Mentioned previous theoretical studies [4, 11] were performed within the density functional theory (DFT) framework [12] with the standard local density approximation (LDA) and generalized gradient approximation (GGA), which are known by their underestimation of the band gaps of semiconductor and insulator materials [13]. Indeed, DFT with the common LDA and GGA yields satisfactory structural parameter values that are in good agreement with the experimental ones, but it provides unsatisfactory electronic properties, such as the band gap and effective masses. Calculated band gap values using DFT with the common LDA and GGA are likely to be approximately 30–50% smaller than the corresponding experimental ones [14].

Currently, some approximations beyond the LDA and GGA, such as GW, hybrid functionals (B3LYP, Heyd-Scuseria-Ernzerhof (HSE)…), LDA + U, LDA + DMFT dynamical mean-field theory (DMFT), have been developed to better describe the electronic structures of semiconductors and insulators. However, some of these methods are computationally expensive or not satisfactory in all cases [15]; for example, the LDA + U method can only be applied to correlated and localized electrons. Fortunately, a very elegant approach; the so-called Tran–Blaha modified Becke–Johnson (TB-mBJ) potential, has recently been suggested by Tran and Blaha [16–18] to solve this dilemma. The TB-mBJ is an alternative method to obtain a band gap close to the experimental value without being computationally, expensive, unlike the other aforementioned methods. For spinel oxides, the TB-mBJ method has been demonstrated to yield band gaps that are consistent with the more accurate results obtained using the GW method [19, 20]. Tran and Blaha demonstrated that the TB-mBJ potential yields band gaps that are consistent with the experimental values with typical errors of less than 10% for some semiconductors and insulators [15]. The drawback of the TB-mBJ potential is that it cannot be obtained as the derivative of an exchange-correlation energy function [15]. Therefore, this potential cannot be used to calculate properties that depend on energy such as the structural properties.

In this work, we aim to calculate the electronic and optical properties of the $GeMg_2O_4$, $GeZn_2O_4$ and $GeCd_2O_4$ compounds using the GGA-PBEsol [21], Engel–Vosko scheme [22] of the GGA (GGA-EV) and TB-mBJ potential [16–18]. In addition, we aim to demonstrate the advantage of the TB-mBJ method for describing the electronic structure of the considered materials.

2. METHODOLOGY

In the present work, all electronic total energy calculations were performed in the framework of density functional theory (DFT) using the full potential (all-electron) linearized augmented plane wave plus local orbitals (FP-LAPW + lo) method as implemented in the WIEN2k code. In this method, the wave functions are expanded in a linear combination of radial functions time spherical harmonics inside the non-overlapping muffin-tin spheres surrounding each atom and in plane waves in the interstitial region between the spheres. The radii of the muffin-tin spheres (R_{MT}) were taken as large as possible without overlapping spheres. The maximum l for the expansion of the wave function in spherical harmonics inside the muffin-tin spheres was $l_{max} = 10$. A plane-wave cut-off parameter $K_{max} = 4.0$ a.u^{-1} was chosen for the expansion of the wave functions in the interstitial region. The integration over the Brillouin zonewas replaced by a summation on a Monkhorst-Pack grid of $10 \times 10 \times 10$ (47 k-points in the irreducible Brillouin zone (IBZ)). The self-consistent calculations were considered converged when the total energy of the system is stable within 10^{-5} Ry. The atomic positions were relaxed until the forces were below 0.5 mRy a.u^{-1}. The exchange-correlation interaction for the structural properties was treated using the GGA-PBEsol functional [21]. For the electronic properties, in addition to the GGA-PBEsol, the GGA-EV [22] and TB-mBJ [16–18], which better describe the electronic structures of semiconductors and insulators, were applied.

3. RESULTS AND DISCUSSION

3.1. Electronic Properties

Now, we discuss our results regarding the electronic properties of $GeMg_2O_4$, $GeZn_2O_4$ and $GeCd_2O_4$ via the energy bands and density of states. The electronic band structures were calculated at the optimized crystalline structure parameters for the three considered compounds using three different exchange-correlation functionals: the GGA-PBEsol, GGA-EV and TB-mBJ. It is well known that the standard GGA usually severely underestimates the band gap value [23]. Engel and Vosko [22] developed a new GGA version (denoted here as EV-GGA) in order to provide a better estimation of the exchange-correlation potential and consequently a better estimation of the band gap value. This approach (EV-GGA) yields better band splitting and some other properties that mainly depend on the accuracy of the exchange-correlation potential. The recently proposed Tran–Blaha modified Becke–Johnson (TB-mBJ) potential [16–18], as implemented in Wien2K, yields band gap values in better agreement with the experimental ones, with a typical errors less than 10% for some semiconductors and insulators [15].

Calculated energy band dispersions along the high symmetry lines of the Brillouin zone using both the GGA08 and TB-mBJ approaches are depicted in Figure 1 for

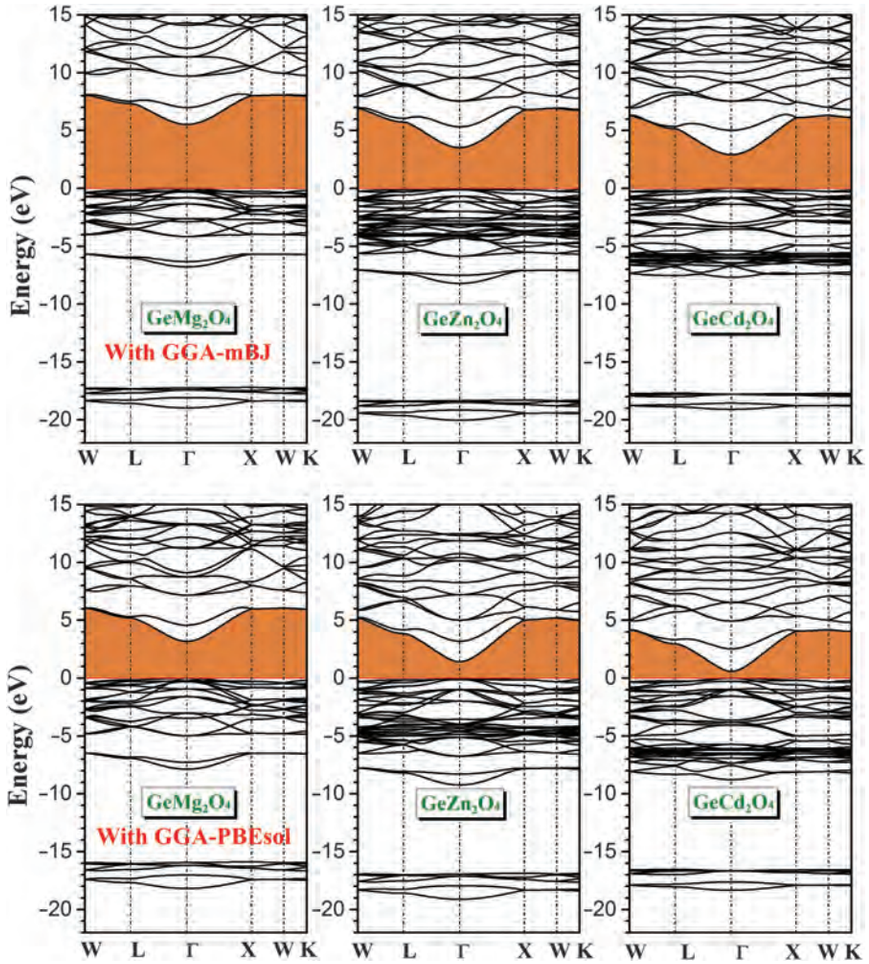

Fig. 1. Band energy dispersions along the high-symmetry directions as calculated using the GGA-PBE sol and TB-mBJ functionals for the spinel oxides $GeMg_2O_4$, $GeZn_2O_4$ and $GeCd_2O_4$. The Fermi level is shifted to zero.

the sake of comparison. In general, the TB-mBJ potential causes a rigid displacement of the conduction bands toward higher energy with small differences in the dispersion at some regions of the Brillouin zone. Both the maximum of the valence band (VBMa) and the minimum of the conduction band (CBMi) are located at Γ-point (Brillouin zone center) for the three studied compounds, allowing us to classify these spinel oxides as direct band gap materials. Calculated fundamental band gaps for the considered materials using three different functionals (GGA-PBEsol, GGA-EV and TB-mBJ) are listed in Table I along with previous theoretical results for comparison. Calculated direct energy band gaps (Γ–Γ) using the GGA-PBEsol method compare favourably to those obtained previously using the same functional [11, 24]. Experimental band gap values for the studied oxides are not yet available to be compared to our predicted values. However, we can assess the obtained results through the accuracy limit of the used functionals. Knowing that calculated band gap values using the DFT with the standard GGA are likely approximately 30–50% smaller than the experimental one [25], one can appreciate that the calculated band gap values using the TB-mBJ potential are significantly improved. Calculated fundamental band gap values using the TB-mBJ approach for the considered oxides are in the range 2.91–5.53 eV. Hence, these materials can be classified as wide-band-gap solids and are consequently transparent in the visible spectra. From the band structures, one can observe that the maxima of the valence bands are flat, indicating that they should have large hole effective masses. Thus, the *p*-type materials should have some unusual transport properties.

To access the nature of electronic states that form the energy bands of the $GeMg_2O_4$, $GeZn_2O_4$ and $GeCd_2O_4$ compounds, their total and partial densities of states (TDOS and PDOS) were explored using the TB-mBJ. Calculated TDOS and PDOS diagrams of $GeMg_2O_4$, $GeZn_2O_4$ and $GeCd_2O_4$ are depicted in Figure 2. Because the DOS diagrams of the three considered compounds are similar, we detail only the density of states of $GeMg_2O_4$

Table I. Some direct and indirect band gap values and the *UVBW* for the $GeMg_2O_4$, $GeZn_2O_4$ and $GeCd_2O_4$ compounds, using the GGA-PBEsol, GGA-EV and Tb-mBJ methods. All energies are in eV.

	Γ–Γ	L–L	X–X	K–K	W–W	Γ–L	Γ–X	Γ–K	Γ–W	*UVBW*
$GeMg_2O_4$										
GGA-PBEsol	3.184	5.371	6.250	6.154	6.456	5.212	5.983	5.957	6.057	7.865
GGA-EV	4.032	6.008	6.797	6.690	6.956	5.861	6.548	6.507	6.596	7.473
TB-mBJ	5.530	7.492	8.280	8.174	8.435	7.341	8.027	7.988	8.089	6.783
Others	3.81[a], 5.8[b], 3.13[c]									
$GeZn_2O_4$										
GGA-PBEsol	1.424	4.018	5.182	5.138	5.518	3.858	5.042	5.008	5.213	9.229
GGA-EV	2.139	4.527	5.569	5.487	5.805	4.382	5.441	5.367	5.535	8.792
TB-mBJ	3.534	5.882	6.939	6.872	7.180	5.750	6.808	6.760	6.941	8.210
Others	1.91[a], 3.9[b], 1.28[c]									
$GeCd_2O_4$										
GGA-PBEsol	0.585	3.209	4.254	4.226	4.498	2.961	4.064	4.038	4.171	8.781
GGA-EV	1.431	3.940	4.942	4.752	5.201	3.717	4.769	4.752	4.913	8.446
TB-mBJ	2.916	5.349	6.300	6.294	6.569	5.156	6.132	6.144	6.312	7.684
Others	0.82[a], 1.8[b], 0.47[c]									

Notes: [a]Ref. [11], [b]Ref. [30] and [c]Ref. [31].

as prototype. The lower group of valence bands, which are not shown for clarity of the figure, extending between −39.6 eV and −39.04 eV, is due to the Mg-*2p* states. The structure localized between −23.21 eV and −22.58 eV is due to the Ge-*d* states. The structure localized between −19.13 eV and −17.06 eV mainly consists of the O-*2s* states with a small contribution from the Mg-3*s* and Ge-3*s*3*p* states. The region near the Fermi level, i.e., the top

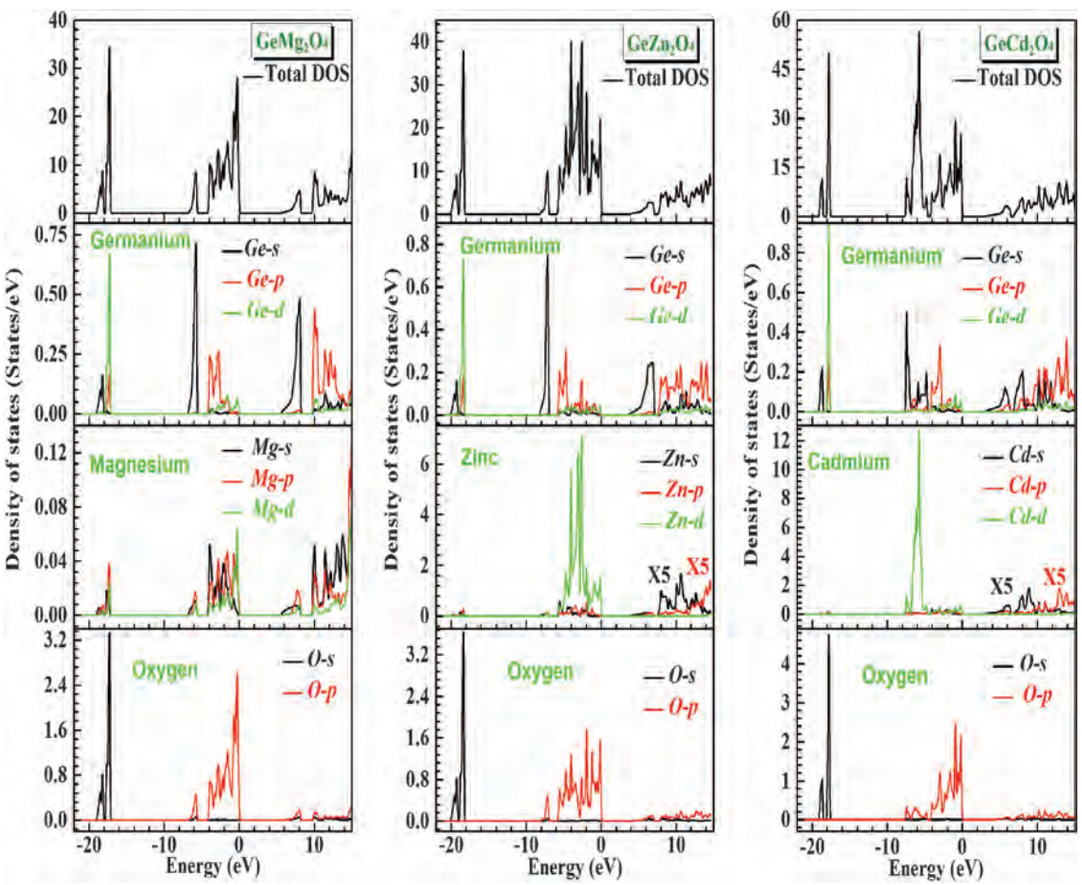

Fig. 2. Diagrams of the total and site-projected densities of states as calculated using the TB-mBJ functional for the spinel oxides $GeMg_2O_4$, $GeZn_2O_4$ and $GeCd_2O_4$. The Fermi level is shifted to zero.

of the valence band, extending between −6.94 eV and 0 eV, is predominantly formed by the O-2*p* states. The substitution of Mg by Zn (Cd) in the $GeZn_2O_4$ ($GeCd_2O_4$) compound introduces a contribution from the Zn-3*d* (Cd-4*d*) states to the upper valence band. Rather than the O-2*p* dominated states in $GeMg_2O_4$, the zinc 3*d* states (cadmium 4*d* states) appear in the upper valence band of $GeZn_2O_4$ ($GeCd_2O_4$); consequently, its width broadens to 8.39 eV. Therefore, changes in the electronic properties of $GeZn_2O_4$ ($GeCd_2O_4$) compared with those of $GeMg_2O_4$ would be solely attributed of the mixing of the Zn-3*d* (Cd-4*d*) and O-2*p* orbitals. In the three compounds, the bottom of the conduction band is composed of the *s* and *p* states of the Ge and B (B = Mg, Zn and Cd) atoms.

Generally, a decrease of the band gap value is expected when a cation is substituted by another heavier cation (e.g., Mg by Zn and Zn by Cd) in a series of structurally isomorphous compounds [22]. We find that the band gap value decreases according to the following sequence: E_g ($GeMg_2O_4$) > E_g ($GeZn_2O_4$) > E_g ($GeCd_2O_4$) (see Table I). The role of the *d* states in defining the electronic properties of the II–VI semiconductors [26], zinc aluminates [4], zinc aluminates, zinc gallate [27] and cubic spinels AB_2O_4, where A = Si and Ge, and B = Mg, Zn and Cd [11, 28], has been discussed. It has been reported that the *p*–*d* hybridization at Γ-point repels the valence band maximum upwards without affecting the conduction band minimum. Hence, the decrease of the calculated direct band gap Γ–Γ from 5.53 eV in $GeMg_2O_4$ to 3.534 eV in $GeZn_2O_4$ and to 2.916 eV in $GeCd_2O_4$ (using TB-mBJ) can be attributed to the presence of the 3*d* and 4*d* states in $GeZn_2O_4$ and $GeCd_2O_4$, respectively.

3.2. Optical Properties

Calculated imaginary parts $\varepsilon_2(\omega)$ of the dielectric functions for the studied compounds using the TB-mBJ potential in the energy range 0–30 eV are presented in Figure 3. It would be of fundamental interest to identify the electronic transitions that are responsible for the peaks and structures in the optical spectra. The imaginary part of the dielectric function is determined by the allowed electronic transitions between each pair of occupied and unoccupied bands. Therefore, the origins of different peaks and features of the optical spectra can be determined by decomposing each spectrum to its individual pair contribution, i.e., the contribution from each electronic transition from an occupied valence state V_i to an empty conduction state C_j ($V_i \rightarrow C_j$) and then plotting the electronic transition energy $E_{ij} = E_{C_j}(k) - E_{V_i}(k)$ along the high-symmetry directions in the Brillouin zone. This technique informs us about the bands that contribute more to the peaks of the $\varepsilon_2(\omega)$ spectrum and their locations in the Brillouin zone. The main contributions to the optical spectra originate from the top valence bands to the lower conduction bands. Because $\varepsilon_2(\omega)$ spectra of the three considered compounds

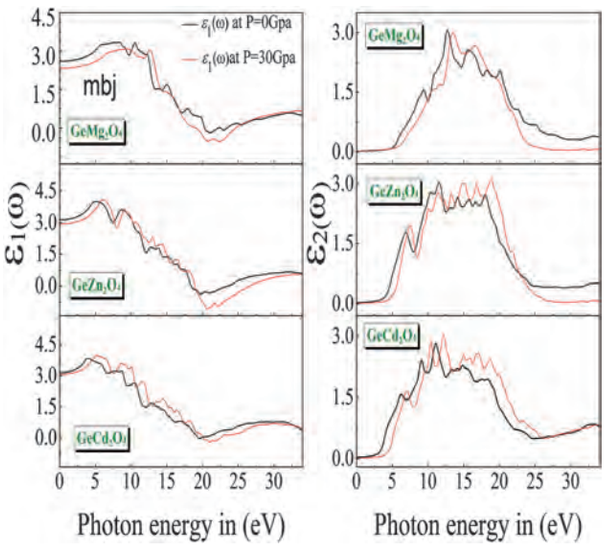

Fig. 3. Real (left panel; $\varepsilon_1(\omega)$) and imaginary (right panel; $\varepsilon_2(\omega)$) parts of the dielectric functions as calculated of the spinel oxides $GeMg_2O_4$, $GeZn_2O_4$ and $GeCd_2O_4$ using the TB-mBJ functional.

are notably similar, we discuss only the decomposition of the $\varepsilon_2(\omega)$ spectrum of $GeMg_2O_4$. The top panel in Figure 4 shows the dominant contributions of the interband transitions to $\varepsilon_2(\omega)$, and the bottom panel shows the locations of these transitions in the Brillouin zone. The first critical point E_0 is the optical absorption edge. This point is the $\Gamma_V - \Gamma_C$ splitting, which gives the threshold of the direct optical transition between the topmost valence band V_1 and the bottommost conduction band C_1 ($V_1 \rightarrow C_1$ transition); the counting of bands is down (up) from the top (bottom) of the valence (conduction) band. This edge is known as the fundamental absorption edge. A broad shoulder appearing at approximately 7.5–11 eV is due to V_3-C_1, V_1-C_1, V_4-C_1 and V_2-C_1 transitions and some other structures centered at E_i points follow this first critical point. Positions of the $\varepsilon_2(\omega)$ peaks together with the dominant interband transitions and their locations in the Brillouin zone for $GeMg_2O_4$ are reported in Table II. We note that all structures in the $\varepsilon_2(\omega)$ spectrum shift toward lower energy when one moves from $GeMg_2O_4$ to $GeZn_2O_4$ to $GeCd_2O_4$. This trend may attributed to the decrease of the band gap value when one moves in the same sequence: $GeMg_2O_4$ to $GeZn_2O_4$ to $GeCd_2O_4$.

The dispersive parts $\varepsilon_1(\omega)$ of the dielectric functions for $GeMg_2O_4$, $GeZn_2O_4$ and $GeCd_2O_4$, which were calculated from the corresponding $\varepsilon_2(\omega)$ using Kramers–Kronig dispersion relation are shown in Figure 3. The static dielectric constant $\varepsilon(0)$ is given by the low energy limit of $\varepsilon_1(\omega)$, i.e., $\varepsilon(0) = \varepsilon_1(\omega \rightarrow 0)$. Calculated static dielectric constants $\varepsilon(0)$ for the considered materials are listed in Table III. One notes that $\varepsilon(0)$ value increases with decreasing band gap E_g. This result is in accordance with Penn model [29]. Penn model is based on the expression

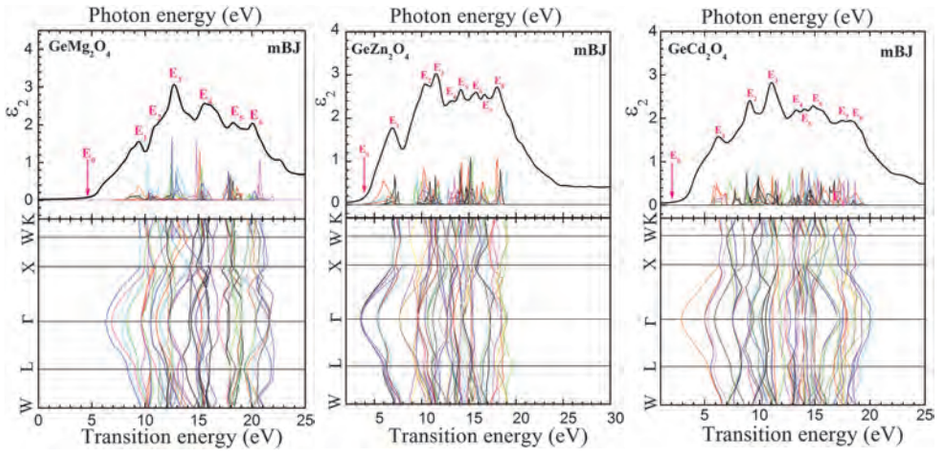

Fig. 4. Decomposition of the imaginary part $\varepsilon_2(\omega)$ of the dielectric function into band-to-band contributions and transition energy band structures for $GeMg_2O_4$, $GeZn_2O_4$ and $GeCd_2O_4$.

$\varepsilon(0) \approx 1 + (\hbar\omega_p/E_g)^2$, where $\hbar\omega_p$ is the plasma energy; $\varepsilon(0)$ is inversely proportional to E_g. Hence, a smaller E_g yields a larger $\varepsilon(0)$.

When the studied compounds are compressed, the positions of all previously mentioned critical points are shifted toward high energy. This behavior can be attributed to the enhancement of the direct band gap under pressure effect. Although their positions are shifted under pressure, the critical points still have the same origins as that at zero pressure. Figure 5 shows pressure dependence of the static dielectric constant $\varepsilon_1(0)$ for the studied compounds. In Figure 5, symbols show the results obtained from *ab-initio* calculation at a given pressure, while the lines are adjustments of the results to second-order polynomials.

Table II. Positions of the $\varepsilon_2(\omega)$ peaks together with the dominant interband transitions and their locations in the Brillouin zone for $GeMg_2O_4$.

Optical structures		Dominant interband transition contributions			
Structure	Peak position	Transition	Region	Percentage	Energy (eV)
E_1	9.40	(V_9–C_1)	W–L, Γ–X	3,7013	9.35
		(V_9–C_2)	W–L, Γ–X	9,74026	9.33
E_2	10.82	(V_1–C_4)	W–L–Γ–X–W–K	11,36364	10.48
		(V_1–C_5)	L–Γ, X–W	15,15152	10.99
		(V_2–C_3)	W–L–Γ–X–W	16,66667	10.35
E_3	12.70	(V_1–C_7)	L–Γ–X–W	6,37255	12.13, 12.76
		(V_1–C_8)	W–L, Γ–X–W–K	5,39216	12.89
		(V_1–C_9)	L–Γ–X	7,35294	12.89
E_4	15.58	(V_1–C_{11})	W–L–Γ–X–W	9,27734	14.80
		(V_1–C_{12})	W–L, Γ–X–W	12,20703	15.05
		(V_1–C_{13})	W–L, Γ–X–W–K	8,30078	15.31
E_5	18.27	(V_{13}–C_{17})	W–L–Γ–X, W–K	5,82353	17.87
		(V_{13}–C_{18})	L–Γ–X	3,79412	17.85
		(V_{17}–C_{12})	L–Γ–X–W–K	7,05882	17.56
E_6	20.07	(V_{17}–C_{21})	W–L, Γ–X–W–K	3,13725	19.83
		(V_{17}–C_{22})	W–L–Γ–X	4,70588	20.36
		(V_{17}–C_{23})	W–L–Γ, X–W–K	8,82353	20.60

The adjustments of the static dielectric constants ($\varepsilon_1(0)$) of the studied compounds to a quadratic polynomial are given by the following expressions:

$$GeMg_2O_4: \varepsilon_1(0) = 2.6018 - 0.01046P + 5.3864 \times 10^{-5}P^2$$

$$GeZn_2O_4: \varepsilon_1(0) = 3.1326 - 0.01130P + 4.8537 \times 10^{-5}P^2$$

$$GeCd_2O_4: \varepsilon_1(0) = 3.1459 - 0.00740P + 3.1050 \times 10^{-5}P^2$$

Calculated refractive index $n(\omega)$ and extinction coefficient $k(\omega)$ as functions of photon energy for the investigated compounds are displayed in Figure 6. For lower energy, the refractive index value is almost constant and begin to increase at energy near the absorption edge to attain a maximum value; then, it decreases for higher energy. The static refractive index $n(0)$ value and energy when dispersion is null E ($n = 1$) for each studied compound are listed in Table III. The static refractive index $n(0)$ value increases when one moves from $GeMg_2O_4$ to $GeCd_2O_4$, following a trend opposite to that of the band gap (the band gap decreases when one moves from $GeMg_2O_4$ to $GeCd_2O_4$). The refractive index attains a maximum value of 1.875 at 10.63 eV for $GeMg_2O_4$, 2.013 at 5.21 for $GeZn_2O_4$ and 1.967 at 4.07 eV for $GeCd_2O_4$. Pressure derivative of the static refractive index $n(0)$ was determined using a linear fit, and the results are listed in Table III. As shown in this table, the refractive index decreases with increasing pressure.

Table III. Calculated static dielectric constant $\varepsilon_1(0)$, static refractive index $n(0)$, and pressure coefficients of the refractive index $n(0)$ for the $GeMg_2O_4$, $GeZn_2O_4$ and $GeCd_2O_4$ compounds.

System	$\varepsilon_1(0)$	$n(0)$	E ($n=1$)	$\frac{1}{n_0}\frac{dn}{dp}(10^{-5}(\text{GPa})^{-1})$
$GeMg_2O_4$	2.603	1.613	20.23	−2.57
$GeZn_2O_4$	3.135	1.770	18.42	−2.69
$GeCd_2O_4$	3.145	1.773	19.39	−2.76

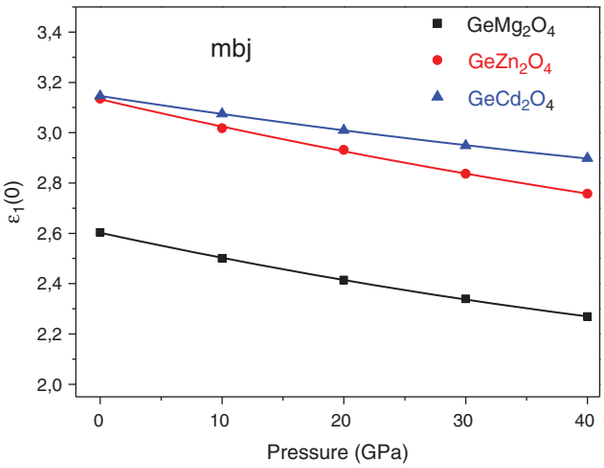

Fig. 5. Pressure dependence of the static dielectric constant $\varepsilon_1(0)$ for the spinel oxides $GeMg_2O_4$, $GeZn_2O_4$ and $GeCd_2O_4$.

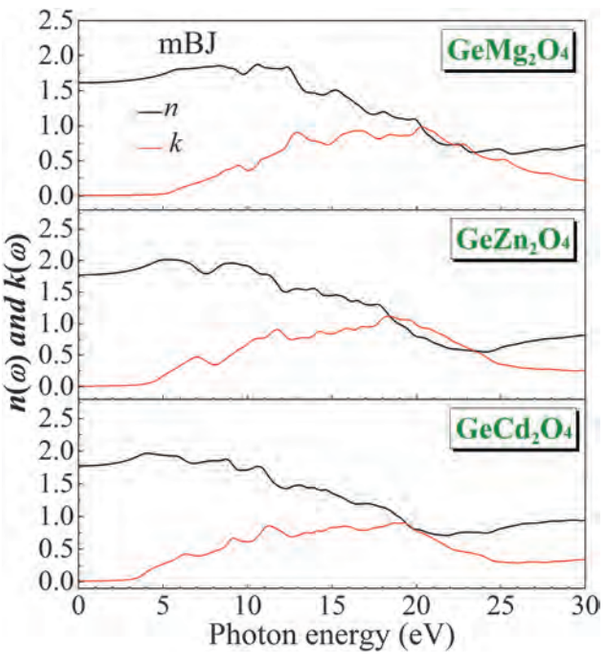

Fig. 6. Refractive index $n(\omega)$ and extinction coefficient $k(\omega)$ as calculated using the TB-mBJ functional for the spinel oxides $GeMg_2O_4$, $GeZn_2O_4$ and $GeCd_2O_4$.

4. CONCLUSION

We have used the FP-LAPW + lo method to explore the structural, electronic and optical properties of the spinel oxides $GeMg_2O_4$, $GeZn_2O_4$ and $GeCd_2O_4$. We investigated the electronic properties using three different functionals: GGA-PBEsol, GGA-EV and TB-mBJ. We find that the TB-mBJ functional significantly improves the electronic structure results compared to the other used functionals. Both VBMa and CBMi are located at Γ point, therefore, the studied spinel oxides are direct band gap materials. The fundamental energy band gap increases with increasing pressure and fit well to a quadratic polynomial for all considered compounds. The bottommost of the CB is dispersive, whereas the topmost of the VB is less dispersive. Consequently, the mobility of the VB holes should be lower than that of CB electrons. The fundamental band gap value decreases when one moves from $GeMg_2O_4$ to $GeZn_2O_4$ to $GeCd_2O_4$. Optical functions, including dielectric function, refractive index, and extinction coefficient, were predicted for a wide energy range 030 eV. Decomposing the imaginary part of the dielectric function into individual band-to-band contributions and plotting the transition energy have allowed us to identify the microscopic origin of the features in the optical spectra. We find that $\varepsilon_1(0)$ increases with decreasing band gap, which is in agreement with Penn model.

References and Notes

1. Sonehara, T., Kato, K., Ozaka, K., Takata, M. and Katsufuji, T., **2006**. Transport, magnetic, and structural properties of spinel $MnTi_2O_4$ and the effect of V doping. *Phys. Rev. B, 74*, p.104424.
2. Okeke, U.O. and Lowther, J.E., **2008**. Theoretical electronic structures and relative stabilities of the spinel oxynitrides M_3NO_3 (M = B, Al, Ga, In). *Phys. Rev. B, 77*, p.094129.
3. Segev, D. and Wei, S.H., **2005**. Structure-derived electronic and optical properties of transparent conducting oxides. *Phys. Rev. B, 71,* p.12529.
4. Wei, S.H. and Zhang, S.B., **2001**. First-principles study of cation distribution in eighteen closed-shell $A^{II}B^{III}_2O_4$ and $A^{IV}B^{II}_2O_4$ spinel oxides. *Phys. Rev. B, 63,* p.045112.
5. Bouhemadou, A., Khenata, R. and Zerarga, F., **2007**. *Ab initio* study of the structural and elastic properties of spinels MgX_2O_4 (X = Al, Ga, In) under pressure. *Eur. Phys. J. B, 56*, pp.1–5.
6. Bouhemadou, A., Allali, D., Boudiaf, K., Al Qarni, B., Bin-Omran, S. and Khenata, R., **2018**. Electronic, optical, elastic, thermoelectric and thermodynamic properties of the spinel oxides $ZnRh_2O_4$ and $CdRh_2O_4$. *J. Alloys Compd.*, *774*, pp.299–314.
7. Allali, D., Bouhemadou, A. and Bin-Omran, S., **2012**. Theoretical prediction of the structural, electronic and optical properties of SnB_2O_4 (B = Mg, Zn, Cd). *Comput. Mat. Sci.*, *51*, pp.194–205.
8. Bouhemadou, A., Khenata, R., Zerarga F. and Bin-Omran, S., **2011**. Structural, electronic and optical properties of spinel oxides $ZnAl_2O_4$, $ZnGa_2O_4$ and $ZnIn_2O_4$. *Solid State Sci.*, *13*, pp.1638–1648.
9. Bouhemadou, A., Khenata, R. and Zerarga F., **2007**. Prediction study of structural and elastic properties under pressure effect of CdX_2O_4 (X = Al, Ga, In) spinel oxides. *Comput. Mat. Sci.*, *39*, pp.709–712.
10. Lewis, B.G. and Paine, D.C., **2000**. Applications and processing of transparent conducting oxides. *MRS Bulletin, 25*(8), pp.22–27.
11. Bouhemadou, A., **2008**. Theoretical study of the structural, elastic and electronic properties of the GeX_2O_4 (X = Mg, Zn, Cd) compounds under pressure. *Modeling Simul. Mater. Sci. Eng., 16,* p.055007.
12. Hohenberg, P. and Kohn, W., **1964**. Inhomogeneous electron gas. *Phys. Rev. B, 136*, p.684.
13. Aulbur, W.G., Jönsson, L. and Wilkins, J.W., **2000**. Quasiparticle calculations in solids. *Solid State Phys., 54,* p.1.

14. Karazhanov, S.Zh., Ravindran, P., Fjellvag, H. and Svensson, B.G., **2009**. Electronic structure and optical properties of $ZnSiO_3$ and Zn_2SiO_4. *J. Appl. Phys. 106,* p.123701.

15. Koller, D., Tran, F. and Blaha, P., **2011**. Merits and limits of the modified Becke-Johnson exchange potential. *Phys. Rev. B, 83*, p.195134.

16. Becke, A.D. and Johnson, E.R., **2006**. A simple effective potential for exchange. *J. Chem. Phys., 124*, p.221101.

17. Tran, F. and Blaha, P., **2009**. Accurate band gaps of semiconductors and insulators with a semilocal exchange-correlation potential. *Phys. Rev. Lett., 102*, p.226401.

18. Tran, F., Blaha, P. and Schwarz, K., **2007**. Band gap calculations with Becke–Johnson exchange potential. *J. Phys.: Condens. Matter., 19,* p.196208.

19. Dixit, H., Tandon, N., Cottenier, S., Saniz, R., Lamoen, D., Partoens, B., Van Speybroeck, V. and Waroquier, M., **2011**. Electronic structure and band gap of zinc spinel oxides beyond LDA: $ZnAl_2O_4$, $ZnGa_2O_4$ and $ZnIn_2O_4$. *New Journal of Physics*, *13*, p.063002.

20. Dixit, H., Saniz, R., Cottenier, S., Lamoen, D. and Partoens, B., **2012**. Electronic structure of transparent oxides with the Tran–Blaha modified Becke–Johnson potential. *J. Phys.: Condens. Matter.*, *24*, p.205503.

21. Perdew, J.P., Ruzsinszky, A., Csonka, G.I., Vydrov, O.A., Scuseria, G.E., Constantin, L.A., Zhou, X. and Burke, K., **2008**. Restoring the density-gradient expansion for exchange in solids and surfaces. *Phys. Rev. Lett., 100*, p.136406.

22. Engel, E. and Vosko, S.H., **1994**. Exact exchange-only potentials and the virial relation as microscopic criteria for generalized gradient approximations. *Phys. Rev. B, 47*, p.13164.

23. Dufek, P., Blaha, P. and Schwarz, K., **1994**. Applications of engel and Vosko's generalized gradient approximation in solids. *Phys. Rev. B*, *50*, p.7279.

24. Camargo-Martínez, J.A. and Baquero, R., **2012**. Performance of the modified Becke-Johnson potential for semiconductors. *Phys. Rev. B*, *86*, p.195106.

25. Karazhanov, S.Zh., Ravindran, P., Fjellvag, H. and Svensson, B.G., **2009**. Electronic structure and optical properties of $ZnSiO_3$ and Zn_2SiO_4. *Journal of Applied Physics*, *106*, p.123701.

26. Wei, S.H. and Zunger, A., **1988**. Role of metal *d* states in II–VI semiconductors. *Phys. Rev. B, 37*, p.8958.

27. Sampath, S.K., Kambere, D.G. and Pandey, R., **1999**. Electronic structure of spinel oxides: Zinc aluminate and zinc gallate. *J. Phys. Condens. Matter, 11*, p.3635.

28. Bouhemadou, A. and Khenata, R., **2007**. Calculated structural, elastic and electronic properties of SiX_2O_4 (X = Mg, Zn, Cd) compounds under pressure. *Modeling Simul. Mater. Sci. Eng.*, *15*, p.787.

29. Penn, D.R., **1960**. Wave-number-dependent dielectric function of semiconductors. *Phys. Rev., 128*, p.2093.

30. Manzar, A., Murtaza, G., Khenata, R., Muhammad, S. and Hayatullah, **2013**. Electronic and optical properties of spinel $GeMg_2O_4$ and $GeCd_2O_4$. *Chin. Phys. Lett., 30*, p.127401.

31. Candan, A. and Uğur, G., **2016**. First-principles study of structural, electronic, elastic and phonon properties of AB_2O_4 (A = Ge, Si; B = Mg, Zn, Cd) spinel oxides. *Modern Physics Letters B, 30*(3), p.1650002.